

# High Yield Multiwall Carbon Nanotube Synthesis in Supercritical Fluids

Danielle K. Smith, Doh C. Lee, and Brian A. Korgel\*

Department of Chemical Engineering, Texas Materials Institute, Center for Nano and Molecular Science and Technology, The University of Texas at Austin, Austin, Texas 78712-1062

Received March 10, 2006. Revised Manuscript Received May 9, 2006

Multiwall carbon nanotubes (MWNTs) with outer diameters of 10–50 nm and wall thicknesses of 5–20 nm were synthesized in supercritical toluene at temperatures ranging from 600 to 645 °C at 8.3 MPa. Nanotube formation was catalyzed by metallocenes such as cobaltocene, nickelocene, and ferrocene or cobalt or iron nanocrystals; toluene served as both the solvent and the carbon source for nanotube growth. Supplemental carbon sources, either hexane or ethanol (~30 vol %), increased the yield of the carbon nanotubes relative to pure toluene, and catalytic amounts of water (0.75 vol %) minimized the formation of carbon filaments and amorphous carbon. Cobaltocene, with ethanol as a supplemental carbon source, gave the highest percentage of nanotubes in the product (~70%) and the highest conversion of toluene to MWNTs (~4%). The MWNTs tended to exhibit bamboo morphology and appear to grow by a folded-growth mechanism with graphitic sheets wrapped around the seed metal particles. Cobaltocene was also found to catalyze coiled nanotube formation, with the appearance of springs, hairpins, lassos, and coiled ropes.

## Introduction

Carbon nanotubes are potentially useful in nanoelectromechanical systems and structural/functional composites;<sup>1</sup> they exhibit high mechanical strength and modulus,<sup>2</sup> high electrical conductivity,<sup>3</sup> and high thermal conductivity.<sup>4</sup> Many synthetic approaches to carbon nanotubes exist, including arc discharge, laser ablation, and chemical vapor deposition (CVD), and some of these techniques can produce nanotubes in sizable quantities; however, their high manufacturing costs still prohibit widespread commercialization, particularly in the case of single-walled carbon nanotubes (SWNTs).<sup>5</sup>

Solution-phase synthetic routes have the potential for continuous processing with high precursor concentrations, making them perhaps more scalable than vapor-phase routes. Carbon nanotube synthesis, however, typically requires temperatures much higher than the boiling point of conventional solvents, which makes solution routes difficult to conceive. One approach for reaching high solution temperatures is to pressurize the solvent. In water, for example, multiwall carbon nanotubes (MWNTs) have been made under hydrothermal conditions at 700–800 °C from reactants such as amorphous carbon, polyethylene, ethylene glycol, and poly(ethylene glycol) either in the presence of a catalyst or without one.<sup>6–10</sup> There have been efforts to decrease the reaction temperature needed to generate nanotubes, and

recently a low-temperature hydrothermal MWNT synthesis was reported at 160 °C.<sup>10</sup> MWNTs have also been produced by solvothermal routes (i.e., pressurized *organic* solvents), for example, by catalyzed reduction of ethanol (both the solvent and the carbon source) using metal oxides at 550 °C,<sup>11</sup> hexachlorobenzene using nickel chloride in cyclohexane at 230 °C,<sup>12</sup> hexachlorobenzene using a Co/Ni catalyst in benzene at 350 °C,<sup>13</sup> tetrachloroethylene using metallic potassium in benzene at 200 °C,<sup>14</sup> and the thermal decomposition of ethoxylated alcohol polyoxyethylene at 310 °C using hexane as a solvent without the presence of a catalyst.<sup>15</sup> A benzene thermal reduction catalysis route at 200 °C using tetrachloroethylene with a metallic potassium catalyst<sup>14</sup> and the magnesium reduction of ethanol (both the solvent and the carbon source) at 600 °C have also been reported.<sup>16</sup>

In our laboratory, we recently demonstrated ferrocene-catalyzed MWNT synthesis in supercritical toluene at ~625 °C and 12.4 MPa.<sup>17,18</sup> Toluene serves as both a solvent and

\* Corresponding author: e-mail, korgel@mail.che.utexas.edu; tel., 512-471-5633; fax, 512-471-7600.

- (1) Meyyappan, M. *Carbon Nanotubes: Handbook of Nanoscience, Engineering, and Technology*; CRC Press: Boca Raton, 2003.
- (2) Treacy, M. M. J.; Ebbesen, T. W.; Gibson, J. M. *Nature* **1996**, *381*, 678.
- (3) Ebbesen, T. W.; Ajayan, P. M. *Nature* **1992**, *358*, 220.
- (4) Ruoff, R. S.; Lorents, D. C. *Carbon* **1995**, *33*, 925.
- (5) Baughman, R. H.; Zakhidov, A. A.; de Heer, W. A. *Science* **2002**, *297*, 787.

- (6) Gogotsi, Y.; Libera, J. A.; Yoshimura, M. *J. Mater. Res.* **2000**, *15*, 2591.
- (7) Calderon Moreno, J. M.; Yoshimura, M. *J. Am. Chem. Soc.* **2001**, *123*, 741.
- (8) Libera, J.; Gogotsi, Y. *Carbon* **2001**, *39*, 1307.
- (9) Suchanek, W. L.; Libera, J. A.; Gogotsi, Y.; Yoshimura, M. *J. Solid State Chem.* **2001**, *160*, 184.
- (10) Wang, W.; Huang, J. Y.; Wang, D. Z.; Ren, Z. F. *Carbon* **2005**, *43*, 1328.
- (11) Zhang, W.; Ma, D.; Liu, J.; Kong, L.; Yu, W.; Qian, Y. *Carbon* **2004**, *42*, 2341.
- (12) Hu, G.; Cheng, M.; Ma, D.; Bao, X. *Chem. Mater.* **2003**, *15*, 1470.
- (13) Jiang, Y.; Wu, Y.; Zhang, S.; Xu, C.; Yu, W.; Xie, Y.; Qian, Y. *J. Am. Chem. Soc.* **2000**, *122*, 12383.
- (14) Wang, X.; Lu, J.; Xie, Y.; Du, G.; Guo, Q.; Zhang, S. *J. Phys. Chem. B* **2002**, *106*, 933.
- (15) Wang, W.; Kunwar, S.; Huang, J. Y.; Wang, D. Z.; Ren, Z. F. *Nanotechnology* **2005**, *16*, 21.
- (16) Liu, J.; Shao, M.; Chen, X.; Yu, W.; Liu, X.; Qian, Y. *J. Am. Chem. Soc.* **2003**, *125*, 8088.

a carbon source for nanotube growth. Toluene is chemically stable up to about 650 °C, but metallocenes such as ferrocene catalyze decomposition to carbon and promote nanotube formation at slightly lower temperatures. Therefore, carbon formation occurs only at the catalyst. In the supercritical fluid, the carbon reactant and dispersed metal catalyst concentrations can be orders of magnitude higher than those possible in vapor-phase processes. In our previous work, the yield of MWNTs obtained from supercritical toluene had a low conversion of toluene to carbonaceous product (less than 1%) and low purity; only 2% of the carbon product was nanotubes.<sup>18</sup>

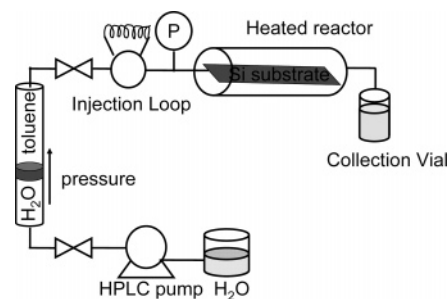
Here, we show that MWNTs can be synthesized with relatively high yield—up to 4% conversion of toluene to MWNTs—in supercritical toluene by using cobaltocene as a catalyst with the addition of ethanol (30 vol %) and catalytic amounts of water (0.75 vol %). Nickelocene, ferrocene, cobaltocene, Co, and Fe nanocrystals all work as catalysts, but cobaltocene gives the highest yields and purity, followed by nickelocene. Relative to these catalysts, ferrocene is actually not very effective. Water was found to be a critical additive, preventing to a large extent amorphous carbon and carbon filament formation. The addition of ethanol increased the yield by almost an order of magnitude relative to pure toluene.

### Experimental Details

**Starting Materials.** Hexane, anhydrous toluene, ferrocene (98%), and cobaltocene were used as received from Aldrich Chemical Co. (Milwaukee, WI). Water was doubly distilled and deionized (DI-H<sub>2</sub>O). Ethanol was purchased from Fisher Scientific (Pittsburgh, PA), and anhydrous nickelocene (97%) was purchased from Fluka (Milwaukee, WI). Anhydrous toluene, ferrocene, cobaltocene, and nickelocene were stored under nitrogen prior to use. Fe nanocrystals were synthesized by thermal decomposition of iron pentacarbonyl (Fe(CO)<sub>5</sub>; Aldrich) in octyl ether (Fluka) and oleic acid (Fluka) at 100 °C.<sup>19</sup> Co nanocrystals were synthesized by the decomposition of dicobalt octacarbonyl (Aldrich, 90–95% Co, stabilized with hexane) in the presence of anhydrous *o*-dichlorobenzene (Aldrich, 99%), oleic acid (Aldrich, 99%), and trioctylphosphine oxide (Strem Chemicals, 99%) at 182 °C.<sup>20</sup>

**MWNT Synthesis.** MWNTs were synthesized using a continuous flow-through process similar to the one we described in ref 21. A high-pressure 10 mL stainless steel vessel (High-Pressure Equipment Co., Erie, PA, HiP) is connected to 1/8 in. o.d. and 0.060 in. size i.d. stainless steel high-pressure tubing (HiP) via stainless steel reducers (HiP) and stainless steel high-pressure valves as shown in Scheme 1. The inlet is connected to a six-way valve (Valco) with a 10 mL injection loop. The outlet is connected to a micrometering valve (HiP). The reactor is pressurized using a high-pressure liquid chromatography (HPLC) pump (Alcott) connected to a piston filled with anhydrous toluene. The piston is pressurized using water to avoid having to run solvent through the HPLC pump. The reactor pressure is measured with a digital pressure gauge

Scheme 1. Supercritical Reactor System



(Sensotech), and the temperature of the brass heating block is monitored with a type K thermocouple and temperature controller (Omega). A silicon wafer cut to 1 cm × 5 cm was placed inside the reactor to facilitate nanotube collection.

The reactor was loaded with toluene, preheated to the reaction temperature (between 600 and 645 °C), and pressurized to 1200 psig (8.3 MPa) with anhydrous toluene. (Extreme caution must be exercised in all reactions close to 650 °C, as these conditions are close to the equipment limitations of the reactor connections.) Catalyst was dissolved in anhydrous toluene, and the supplemental carbon source and DI-H<sub>2</sub>O (if present) were added and vigorously mixed. This reactant solution was then immediately injected from a 10 mL injection loop at a rate of 1 mL/min. As the reaction proceeded, product was collected in a vial at the outlet of the reactor. Reactions were always performed in a fume hood, and the collection vial was sealed yet vented to prevent pressure buildup upon cooling. The reaction was carried out for 10 min before removing the reactor from the heating block and cooling to room temperature. The reactor was then opened under ambient conditions, the deposition substrate was removed, and the remaining loose product of black soot was collected by rinsing with chloroform.

**Purification and Characterization.** The reaction products were characterized by thermogravimetric analysis (TGA), high-resolution scanning electron microscopy (HRSEM), transmission electron microscopy (TEM), and energy-dispersive X-ray spectroscopy (EDS). For HRSEM, the product was imaged on the silicon substrate removed directly from the reactor, and no additional treatment was performed to the substrate or product prior to imaging on a LEO 1530 HRSEM at 3 kV with working distance between 7 and 12 mm using an in-lens detector.

TGA was performed on 10 mg of unpurified cobaltocene-catalyzed MWNTs (synthesized in supercritical toluene at 640 °C and 8.3 MPa with 8.2 mM cobaltocene, 3.7 mM ethanol, and 0.2 mM DI-H<sub>2</sub>O) and 10 mg of an amorphous carbon sample obtained from a failed nanotube reaction placed in an open-top alumina sample pan in a Perkin-Elmer TGA 7. The samples were heated in air to 300 °C at a heating rate of 20 °C/min and allowed to equilibrate for 1 min before being heated from 300 to 900 °C at 1 °C/min. Scan rates higher than 1 °C/min gave slightly elevated decomposition temperatures, as also noted previously by McKee and Vecchio.<sup>22</sup>

For TEM imaging, the nanotubes were treated with nitric acid and hydrogen peroxide to remove residual soot—purification that enabled high-resolution imaging of the nanotubes. Approximately 3 mg of product was refluxed at 120 °C in 10 mL of 7 M nitric acid (Aldrich) for 3 h. The solution was cooled to room temperature and centrifuged at 8000 rpm for 10 min. The supernatant was discarded, and the precipitate was redispersed in DI-H<sub>2</sub>O with brief sonication and centrifuged again. This precipitation/centrifugation step was repeated again to ensure that residual acid, amorphous

(17) Lee, D. C.; Korgel, B. A. *Mol. Simul.* **2005**, *31*, 637.

(18) Lee, D. C.; Mikulec, F. V.; Korgel, B. A. *J. Am. Chem. Soc.* **2004**, *126*, 4951.

(19) Hyeon, T.; Lee, S. S.; Park, J.; Chung, Y.; Na, H. B. *J. Am. Chem. Soc.* **2001**, *123*, 12798.

(20) Puentes, V. F.; Zanchet, D.; Erdonmez, C. K.; Alivisatos, A. P. *J. Am. Chem. Soc.* **2002**, *124*, 12874.

(21) Hanrath, T.; Korgel, B. A. *J. Am. Chem. Soc.* **2002**, *124*, 1424.

(22) McKee, G. S. B.; Vecchio, K. S. *J. Phys. Chem. B* **2006**, *110*, 1179.



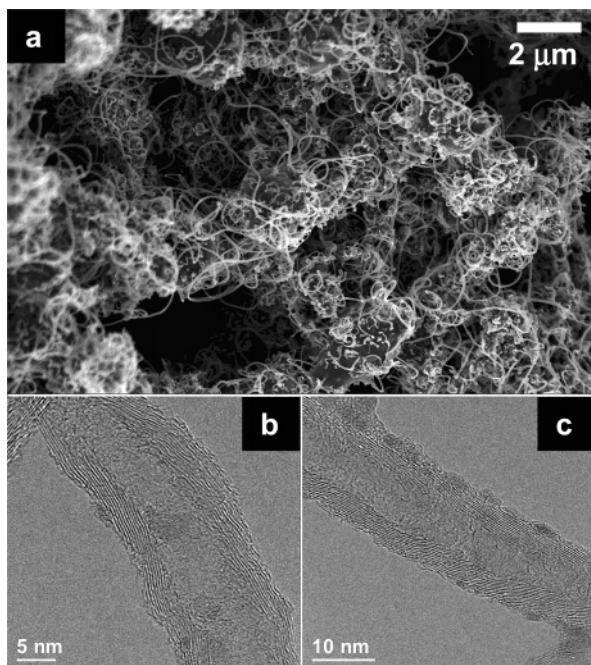


**Figure 1.** MWNTs synthesized in supercritical toluene. (a) SEM image of the product collected on the deposition substrate in the reactor without further purification. (b, c) TEM images showing the MWNT structure of the product.

carbon, and catalyst particles were removed. The nanotubes were then dispersed in a 9% hydrogen peroxide ( $\text{H}_2\text{O}_2$ ) solution and refluxed at 80 °C for 6 h. The solution was cooled to room temperature and centrifuged at 8000 rpm for 10 min. The supernatant was discarded, and the precipitate was redispersed in ethanol and centrifuged again. This precipitation/centrifugation step was repeated again. The nanotubes were then ultrasonicated for 2 h using a Cole Parmer 8891 (Vernon Hills, IL) sonication bath and for 10 min using a Branson Sonifier 250 (Danbury, CT) sonication horn. The horn was set to a duty cycle of 10% with an output control of 2. For TEM imaging, 4  $\mu\text{L}$  of the sonicated nanotube dispersion was dropped onto a lacey carbon-coated TEM grid (Electron Microscopy Sciences). High-resolution transmission electron microscopy (HRTEM) imaging was performed on a JEOL 2010F transmission electron microscope operating at a voltage of 200 kV, and EDS data were obtained on an attached Oxford INCA ED spectrometer. The images were acquired digitally by a GATAN digital photography system.

## Results and Discussion

**Metalloocene-Catalyzed MWNT Growth in Supercritical Toluene.** Figure 1 shows a scanning electron microscopy (SEM) image of MWNTs synthesized in supercritical toluene at 640 °C using cobaltocene as a catalyst. The nanotubes were synthesized with a catalytic amount of water (0.75 vol %) and 30 vol % ethanol. The carbon product consists of some amorphous carbon, but primarily MWNTs as shown in the TEM images in Figure 1b,c. Figure 2 shows SEM images of MWNTs synthesized in supercritical toluene at 640 °C using ferrocene, cobaltocene, and nickelocene as catalysts in reactions carried out with water and ethanol (or hexane, with ferrocene). All three metallocenes catalyze MWNT formation, with toluene serving as both a solvent for the reaction and the primary carbon source for MWNT formation. In the cobaltocene-catalyzed reactions, approxi-

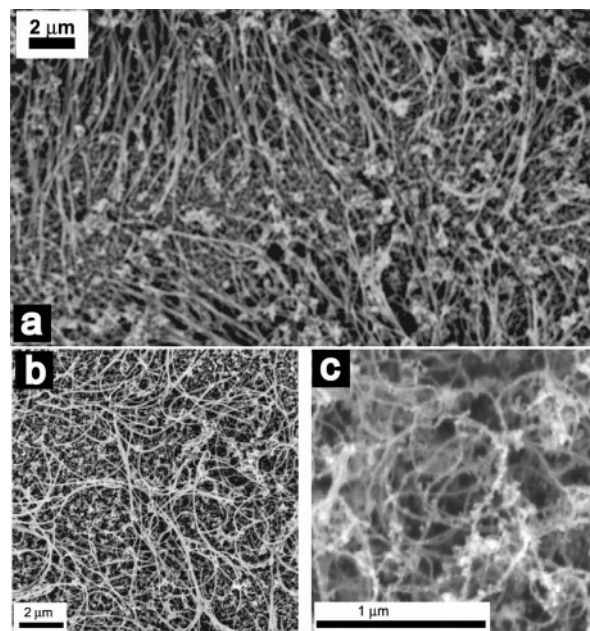


**Figure 2.** HRSEM images of MWNTs synthesized in supercritical toluene at 640 °C and 8.3 MPa with (a) 26 mM ferrocene, 1.6 mM hexane, and 0.2 mM DI- $\text{H}_2\text{O}$ ; (b) 8.2 mM cobaltocene, 3.7 mM ethanol, and 0.2 mM DI- $\text{H}_2\text{O}$ ; and (c) 8.2 mM nickelocene, 3.7 mM ethanol, and 0.2 mM DI- $\text{H}_2\text{O}$ . The reaction product was imaged on the collection substrate taken from the reactor without further purification.

mately 4% of the toluene fed into the reactor was converted to carbonaceous product, and approximately 70% of this product was MWNTs, as determined from SEM. TGA also confirmed that the MWNT product was composed primarily of MWNTs: Figure 3 shows the mass loss profiles and oxidation rates of a MWNT sample compared to an amorphous carbon sample. Amorphous carbon burns off at  $\sim 450$  °C, which is much lower than the MWNT decomposition temperature of  $\sim 630$  °C. Very little decomposition occurs by TGA at temperatures below 500 °C, indicating that the MWNT sample is relatively pure. Further indicating a relatively high purity, the MWNT decomposition temperature is slightly higher than what has previously been reported for MWNTs synthesized by CVD.<sup>22</sup>

The nanotube yield was significantly higher for cobaltocene-catalyzed reactions than for the ferrocene-catalyzed reactions, which converted  $\sim 2\%$  of the toluene into carbon, of which only about 35% of the product was MWNTs. Because toluene serves as the solvent for the reaction, a very high conversion of toluene to nanotubes is not necessarily expected or even desired. This amount of nanotubes, however, is quite significant—approximately 20 mL of toluene gives  $\sim 0.26$  g of MWNTs.

Relative to reactions carried out in pure toluene, ethanol addition significantly increased the yield of MWNTs in cobaltocene- and nickelocene-catalyzed reactions, and small amounts of hexane increased MWNT yields in ferrocene-catalyzed reactions. Mizuno et al.<sup>23</sup> also found that nanotube yields were higher in gas-phase reactions when Fe catalysts were used in conjunction with straight-chain hydrocarbons and when Co catalysts were used in the presence of alcohols. In the supercritical reactions, ethanol and hexane both

(23) Mizuno, K.; Hata, K.; Saito, T.; Ohshima, S.; Yumura, M.; Iijima, S. *J. Phys. Chem. B* **2005**, *109*, 2632.

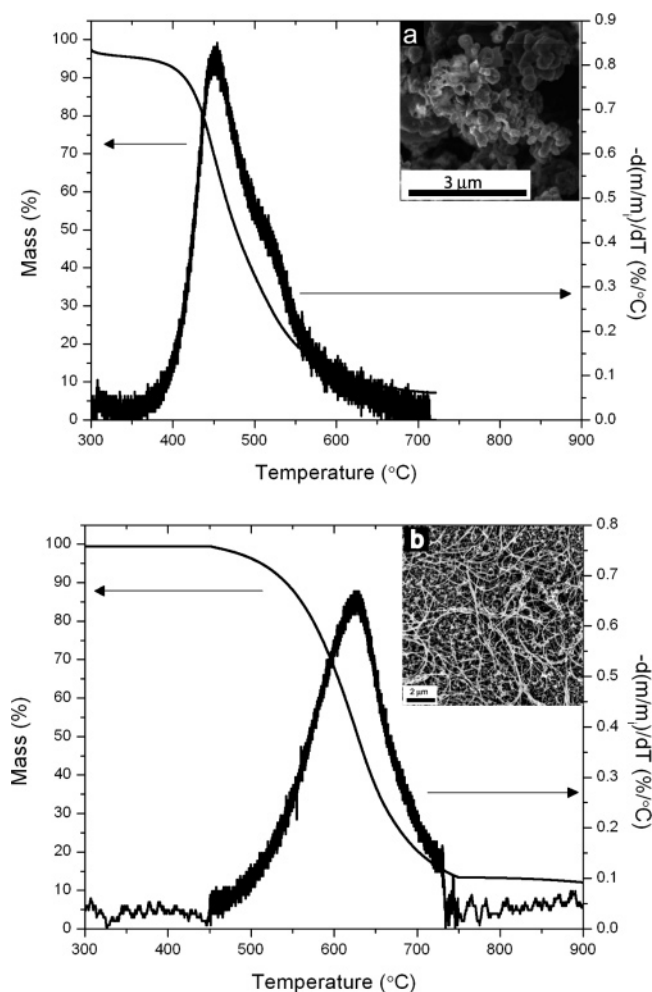


**Figure 3.** TGA of (a) amorphous carbon and (b) MWNTs produced from supercritical toluene reactions. (Insets) SEM images of the analyzed products. The samples were scanned at 1 °C/min. The quantity  $m/m_i$  is the mass fraction of the sample remaining. The peak in  $-d(m/m_i)/dT$  versus  $T$  corresponds approximately to the decomposition temperature of the sample. The absence of significant thermal decomposition below  $\sim 500$  °C in part b indicates that the sample is primarily MWNTs.

decompose much more rapidly than toluene to increase the MWNT yields; however, neither pure hexane nor ethanol when used as the solvent gave good results—hexane in particular is too reactive and decomposes primarily to amorphous carbon. In the case of ethanol,  $-\text{OH}$  radicals may form, increase the toluene decomposition rate, and limit amorphous carbon formation, as Maruyama et al. have suggested in gas-phase reactions using alcohols.<sup>24</sup>

In low concentrations ( $\sim 0.2$ – $4$  mM;  $0.75$  vol %), water greatly reduced the amount of amorphous carbon and carbon filaments formed during the reaction. Below  $\sim 0.1$  mM, water did not improve the purity of the product, whereas concentrations much above  $5$ – $10$  mM poisoned the reaction and prevented nanotube formation. Qualitatively similar results have also been observed in gas-phase carbon nanotube reactions, with water limiting the carbon sidewall deposition and carbonaceous byproduct formation.<sup>25</sup> In the supercritical toluene reactions, water addition was found to be critical to

forming nanotubes at very high temperatures—close to  $650$  °C. In our previous work,<sup>18</sup> nanotube reactions at  $650$  °C using pure toluene gave only amorphous carbon, some filaments, and no observable nanotubes. With the addition of water, a relatively high yield of MWNTs could be obtained in this temperature range. In fact, the highest yield of MWNTs in the presence of water was obtained at  $640$  °C versus  $625$  °C in pure toluene.

Higher catalyst concentrations gave larger amounts of MWNTs. Cobaltocene was the best metallocene catalyst for MWNT growth, giving both the largest amount of MWNTs and the purest product with the highest proportion of carbon nanotubes relative to carbon filaments and amorphous carbon. The mole ratio between Co and C in the nanotubes is approximately 1:1000 in these reactions. Nickelocene produced more MWNTs than ferrocene. In gas-phase reactions, both cobaltocene and nickelocene have catalyzed SWNT synthesis under experimental conditions where ferrocene has not,<sup>26–28</sup> and the yield of SWNTs has been higher with cobaltocene than with nickelocene.<sup>28</sup> Although fundamental understanding of nanotube growth is still being refined, these observations are consistent with expectations based on the C–Co, C–Ni, and C–Fe<sup>29</sup> phase diagrams: at temperatures between  $600$  and  $650$  °C, the carbon solubility is an order of magnitude higher in Co than Ni or  $\alpha$ -Fe, ranging from  $0.1$  to  $0.2$  atomic % in Co down to  $0.0$ – $0.1$  to  $0.01$ – $0.03$  atomic % in Ni and Fe, respectively.

Within a rather narrow temperature range, the MWNT yield increased with higher reaction temperature. At  $600$  °C and below, toluene does not decompose, even in the presence of the catalyst. At temperatures above  $\sim 645$  °C, good quality MWNTs are produced but with excessive amounts of amorphous carbon due to homogeneous toluene decomposition. The highest yield of MWNTs with the least amount of amorphous carbon byproduct was obtained at  $640$  °C. Figures b, c show cobaltocene-catalyzed MWNTs grown at  $640$  °C after purification.

**Fe and Co Nanocrystal-Catalyzed Growth.** Preformed Fe and Co nanocrystals,  $5$ – $6$  nm in diameter, were also studied as catalysts for MWNT synthesis in supercritical toluene. The metallocenes decompose in the reactor to metal particles. This decomposition is relatively uncontrolled, and the final catalyst particle size is limited by many factors such as their decomposition kinetics, concentration, and effect of the nanotubes on metal aggregation. The nanocrystals on the other hand can be injected with a pre-specified size and are reasonably stable during the reaction, although aggregation and coalescence certainly occur to some extent, which increase the size and broaden the size distribution.<sup>30</sup> Somewhat surprisingly, Fe and Co nanocrystals gave significantly lower product yields compared to the metallocenes, by about

- (24) Maruyama, S.; Kojima, R.; Miyauchi, Y.; Chiashi, S.; Kohno, M. *Chem. Phys. Lett.* **2002**, *360*, 229.  
 (25) Futaba, D. N.; Hata, K.; Yamada, T.; Mizuno, K.; Yumura, M.; Iijima, S. *Phys. Rev. Lett.* **2005**, *95*, 056104.

- (26) Satishkumar, B. C.; Govindaraj, A.; Sen, R.; Rao, C. N. R. *Chem. Phys. Lett.* **1998**, *293*, 47.  
 (27) Vivekchand, S. R. C.; Cele, L. M.; Deepak, F. L.; Raju, A. R.; Govindaraj, A. *Chem. Phys. Lett.* **2004**, *386*, 313.  
 (28) Rao, C. N. R.; Govindaraj, A.; Sen, R.; Satishkumar, B. C. *Mater. Res. Innovations* **1998**, *2*, 128.  
 (29) *Binary Alloy Phase Diagrams*, 2nd ed.; ASM International: Materials Park, OH, 1990; Vol. 1.  
 (30) Shah, P. S.; Hanrath, T.; Johnston, K. P.; Korgel, B. A. *J. Phys. Chem. B* **2004**, *108*, 9574.



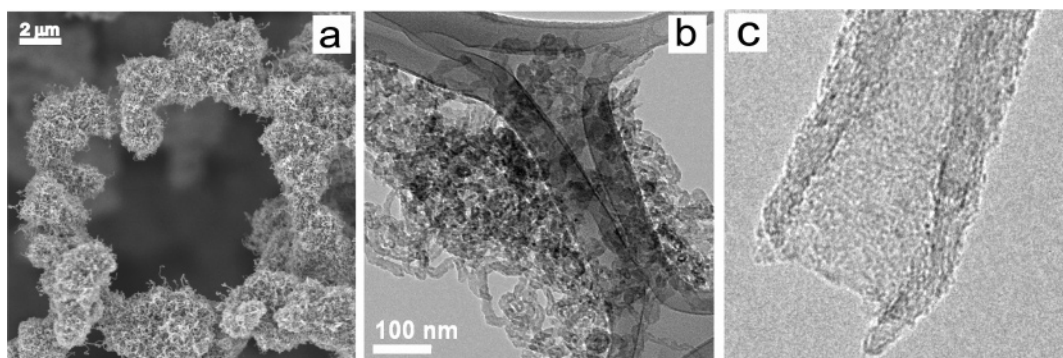


**Figure 4.** Aggregates of nanotubes imaged by (a) SEM and (b) TEM. Purification with nitric acid and hydrogen peroxide solutions and sonication were necessary to obtain better dispersed nanotubes suitable for HRTEM imaging. Very high acid concentrations, greater than  $\sim 16$  M nitric acid, opened and damaged the nanotubes as shown in part c.

an order of magnitude. Perhaps the capping ligand coating on the nanocrystals slows catalytic toluene decomposition at the metal surface. We found recently that the capping ligand coating on Ir nanocrystals significantly influences catalytic reactions, such as the hydrogenation of alkenes, on their surfaces.<sup>31</sup> More study is required to understand the underlying causes for the difference in reaction yields between the nanocrystals and the metallocenes. However, one significant observable difference was the metal seed diameter: the metallocenes were found to decompose into metal particles with diameters of 20–50 nm at the ends of the MWNTs, which are significantly larger than the injected nanocrystals. These observations agree with our previous work in pure supercritical toluene.<sup>18</sup>

**Structural Characterization of the MWNTs.** Nanotubes extracted directly from the reactor were difficult to image by HRTEM. The nanotubes tend to agglomerate and tangle in a matrix of amorphous carbon, as shown in Figure 4. When isolated tubes could be imaged on the TEM grid, they would generally be coated with a few nanometers of amorphous carbon, most likely as a result of sidewall carbon deposition from homogeneously decomposing toluene, similar to what happens in CVD reactions.<sup>32</sup> To obtain HRTEM images, the MWNTs were purified using a process developed by Goto et al.<sup>33</sup> to remove the carbonaceous byproducts. Several other methods were attempted, but this one worked best. Care must be taken to avoid MWNT degradation (see Figure 4c) in the purification process, as noted in the literature for gas-phase produced nanotubes.<sup>34–36</sup>

Very clean HRTEM images could be obtained from the purified MWNTs. For example, Figure 5 shows TEM images of cobaltocene-catalyzed carbon MWNTs. The nanotube walls are composed of ordered graphitic sheets. However, closer examination reveals that the nanotubes exhibit a range of structural defects. Most MWNTs were curly. Cobaltocene-catalyzed MWNTs, for example, exhibited a variety of

interesting shapes, including springs, hairpins, lassos, and coiled ropes (Figure 6). Many nanotubes exhibited kinks, as shown in Figure 7. Often, near these kinks, the inner tube diameter would increase or decrease slightly. Iijima et al.<sup>37,38</sup> have attributed curvature in nanotubes to the addition of either a pentagon or a heptagon into the hexagonal carbon network. These kinds of “point defects” may be the source of the curvature in the MWNTs; however, much more structural characterization is required before such a conclusion can be made. Often, segments in the MWNTs had an orientation angle between the graphite basal planes and the tube axis ( $\theta$ )<sup>39,40</sup> that deviated from zero (Figure 7). In gold nanocrystal-seeded Si nanowire synthesis in supercritical hexane, extended defects occurred as a result of starved growth.<sup>41</sup> To see if the precursor supply rate was too slow and was responsible for the large number of defects in the MWNTs, the flow rate was increased to 1.5 mL/min and both the amount of supplemental carbon source and the reaction temperature were varied independently. No morphology difference was observed in the MWNTs with these changes in the reaction conditions. (MWNTs grown at higher flow rate are shown in Figure 5.) A significant difference in nanotube morphology most likely requires a large change in reaction conditions; for example, Cui et al. showed that significant differences in tube morphology occurred with synthesis temperature differences over a range of 400 °C.<sup>42</sup>

Figure 8 shows TEM images of MWNTs with bamboo morphology—sections of graphite bridge the interior of the nanotube at regular intervals. Bamboo morphology in MWNTs has been observed in many studies and has been attributed in some cases to a root growth mechanism of tubes from metal seed particles.<sup>43–47</sup> The MWNTs synthesized in

(31) Stowell, C. A.; Korgel, B. A. *Nano Lett.* **2005**, *5*, 1203.

(32) Qin, L. C. *J. Mater. Sci. Lett.* **1997**, *16*, 457.

(33) Goto, H.; Furuta, T.; Fujiwara, Y.; Ohashi, T. Method of purifying single wall carbon nanotubes from metal catalyst impurities. U.S. Patent Application 20030007924, January 9, 2003.

(34) Zhang, X.; Sreekumar, T. V.; Liu, T.; Kumar, S. *J. Phys. Chem. B* **2004**, *108*, 16435.

(35) Zhang, M.; Yudasaka, M.; Iijima, S. *J. Phys. Chem. B* **2004**, *108*, 149.

(36) Lee, G.-W.; Kumar, S. *J. Phys. Chem. B* **2005**, *109*, 17128.

(37) Iijima, S.; Ishihashi, T.; Ando, Y. *Nature* **1992**, *356*, 776.

(38) Iijima, S.; Ajayan, P. M.; Ichihashi, T. *Phys. Rev. Lett.* **1992**, *69*, 3100.

(39) Nolan, P. E.; Schabel, M. J.; Lynch, D. C. *Carbon* **1995**, *33*, 79.

(40) Meyyappan, M.; Delzeit, L.; Cassell, A.; Hash, D. *Plasma Sources Sci. Technol.* **2003**, *12*, 205.

(41) Lu, X.; Hanrath, T.; Johnston, K. P.; Korgel, B. A. *Nano Lett.* **2003**, *3*, 93.

(42) Cui, H.; Eres, G.; Howe, J. Y.; Poretzky, A.; Varela, M.; Geoghegan, D. B.; Lowndes, D. H. *Chem. Phys. Lett.* **2003**, *374*, 222.

(43) Liu, J.; Xu, L.; Zhang, W.; Lin, W. J.; Chen, X.; Wang, Z.; Qian, Y. *J. Phys. Chem. B* **2004**, *108*, 20090.

(44) Wang, Y. Y.; Tang, G. Y.; Koeck, F. M.; Brown, B.; Garguilo, J. M.; Nemanich, R. J. *Diamond Relat. Mater.* **2004**, *13*, 1287.

(45) Lee, C. J.; Park, J. *Appl. Phys. Lett.* **2000**, *77*, 3397.

(46) Lee, C. J.; Park, J. H.; Park, J. *Chem. Phys. Lett.* **2000**, *323*, 560.

(47) Lee, C. J.; Park, J. *J. Phys. Chem. B* **2001**, *105*, 2365.

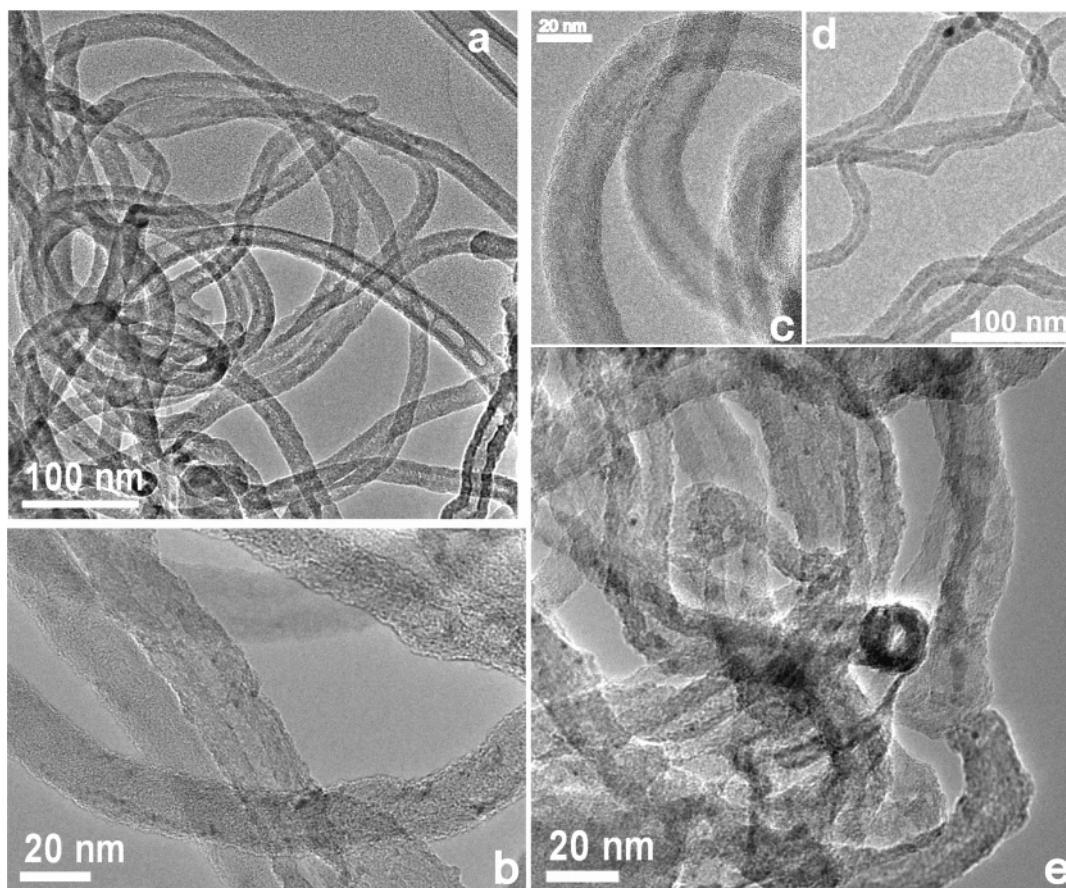


**Figure 5.** HRTEM images of MWNTs. Products obtained from reactions carried out under the following conditions: (a) 0.6 mM cobaltocene, 3.7 mM ethanol, and 0.3 mM DI-H<sub>2</sub>O at 640 °C; (b, d) 8.2 mM cobaltocene, 3.7 mM ethanol, and 0.2 mM DI-H<sub>2</sub>O at 640 °C with a flow rate of 1.5 mL/min; (c) 8.2 mM cobaltocene, 3.7 mM ethanol, and 0.2 mM DI-H<sub>2</sub>O at 640 °C; and (e) 8.2 mM cobaltocene, 3.7 mM ethanol, and 0.04 mM DI-H<sub>2</sub>O at 640 °C. Lower amounts of DI-H<sub>2</sub>O gave more amorphous carbon intermixed with the nanotubes. The quality of the MWNTs did not appear to vary with reactant injection rate.

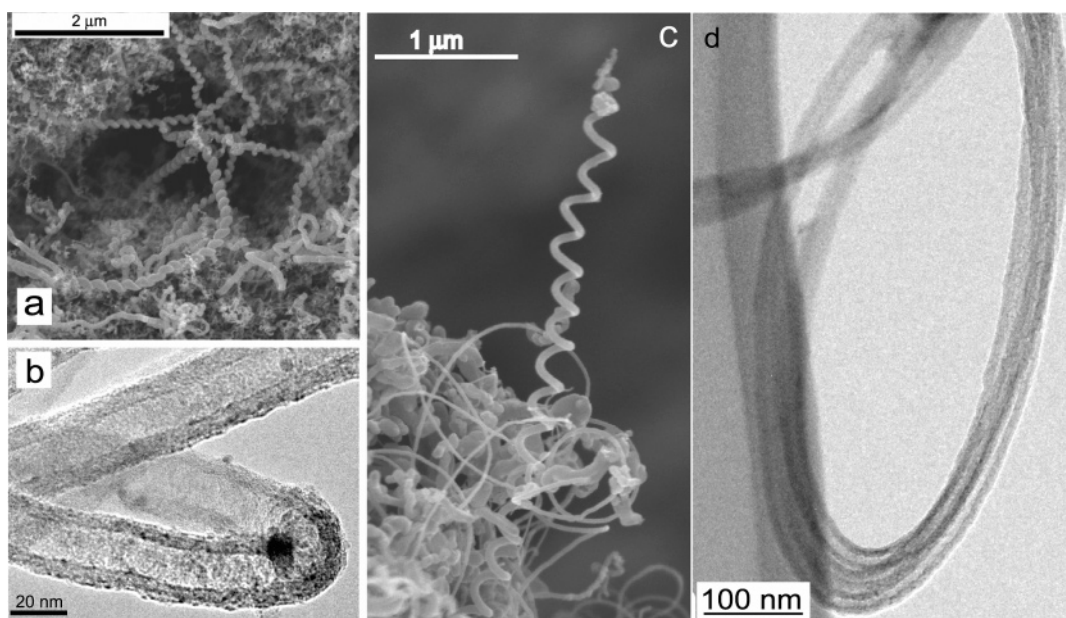


**Figure 6.** Different nanotube structures obtained in cobaltocene-catalyzed reactions: (a) coils (26 mM cobaltocene and 4.9 mM ethanol at 600 °C), (b) hairpins (8.2 mM cobaltocene, 3.7 mM ethanol, and 0.2 mM DI-H<sub>2</sub>O at 640 °C), (c) springs (17 mM ferrocene and 3.7 mM ethanol at 630 °C), and (d) “lassos” (8 mM nickelocene, 3.7 mM ethanol, and 0.2 mM DI-H<sub>2</sub>O at 625 °C).

supercritical toluene from metallocene catalysts, however, appear to grow by a folded-growth mechanism in which at the end of the MWNT the graphite sheets wrap around the

metal seed particle.<sup>17,18</sup> Figure 8 shows several examples of these “folded-growth” structures where the metal seed particle at the tip of the MWNT is coated with graphite.



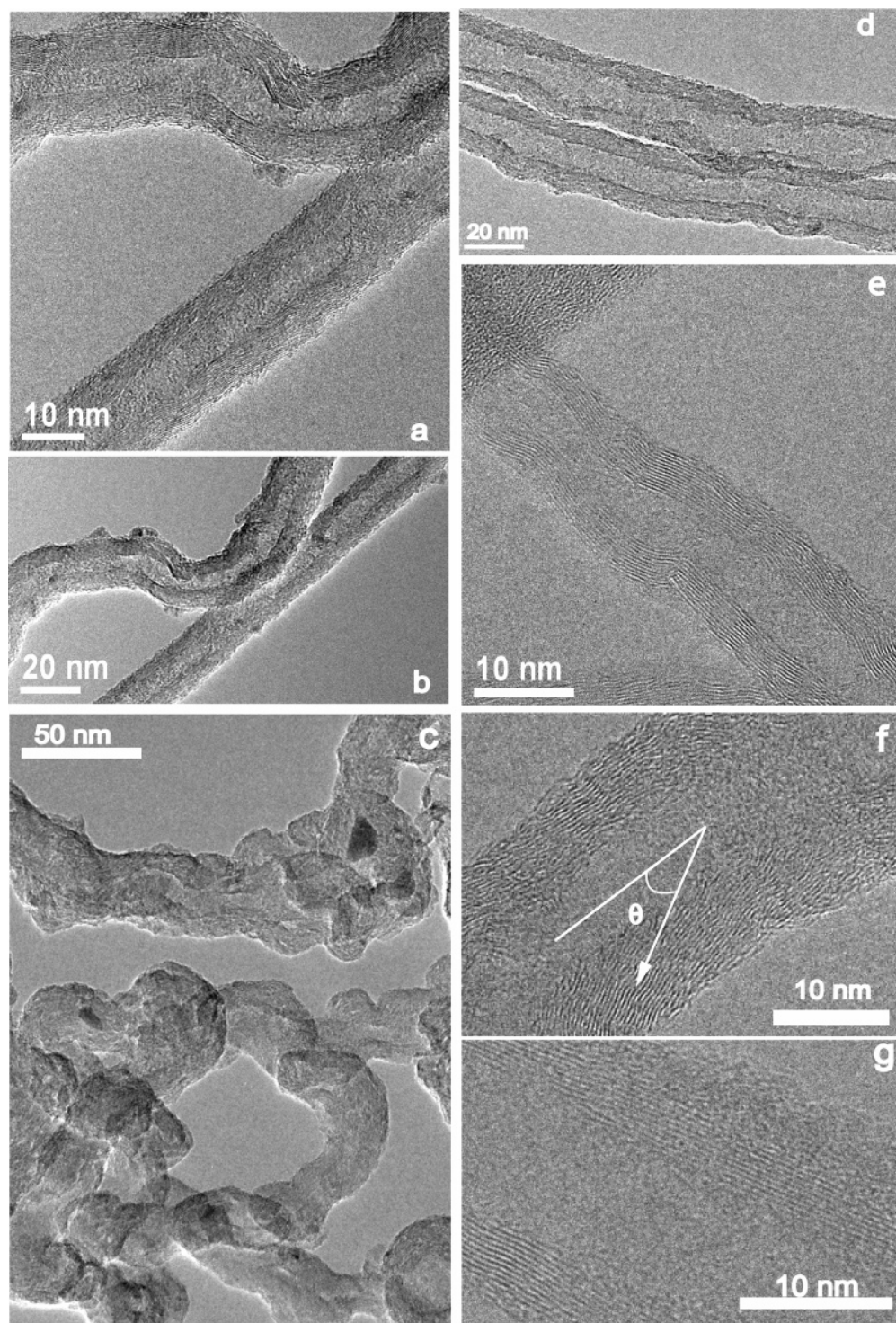


**Figure 7.** HRTEM images showing defects in MWNTs synthesized in supercritical toluene. (a–c) MWNTs synthesized in supercritical toluene with 12 mM cobaltocene, 3.7 mM ethanol, and 4 mM DI-H<sub>2</sub>O at 640 °C. (d) MWNTs synthesized with 8.2 mM cobaltocene, 3.7 mM ethanol, and 0.2 mM water at 640 °C. (e) MWNTs synthesized with 0.6 mM cobaltocene, 3.7 mM ethanol, and 0.3 mM DI-H<sub>2</sub>O at 640 °C. In part f,  $\theta$  is the angle between the tube axis and the graphite basal planes. Nonzero  $\theta$  indicates a defect in the tube wall. Tubes with  $\theta$  equal to zero were also obtained, as shown in part g.

However, it is possible that in some cases the MWNTs might be growing at exposed open ends of the tubes as well, as many nanotubes were observed by TEM with metal catalyst particles embedded in the middle of the nanotubes<sup>48</sup> (Figure 8h). Bamboo morphology in carbon nanotubes has been proposed to be the result of subtle changes in the growth conditions near the seed metal; for example, a fluctuation in

pressure, temperature, or reactant concentration might lead to a defect in the graphite sheet, resulting in a temporary “capping” of the nanotube. Louchev attributed bamboo layer formation to any change in the growth conditions that slows carbon addition to the nanotube edge and gives rise to a high probability of pentagon defect formation,<sup>49</sup> thus resulting in a temporary capping of the tube resulting in the bamboo

(48) Deck, C. P.; Vecchio, K. S. *J. Phys. Chem. B* **2005**, *109*, 12353.

(49) Louchev, O. A. *Phys. Status Solidi A* **2002**, *193*, 585.



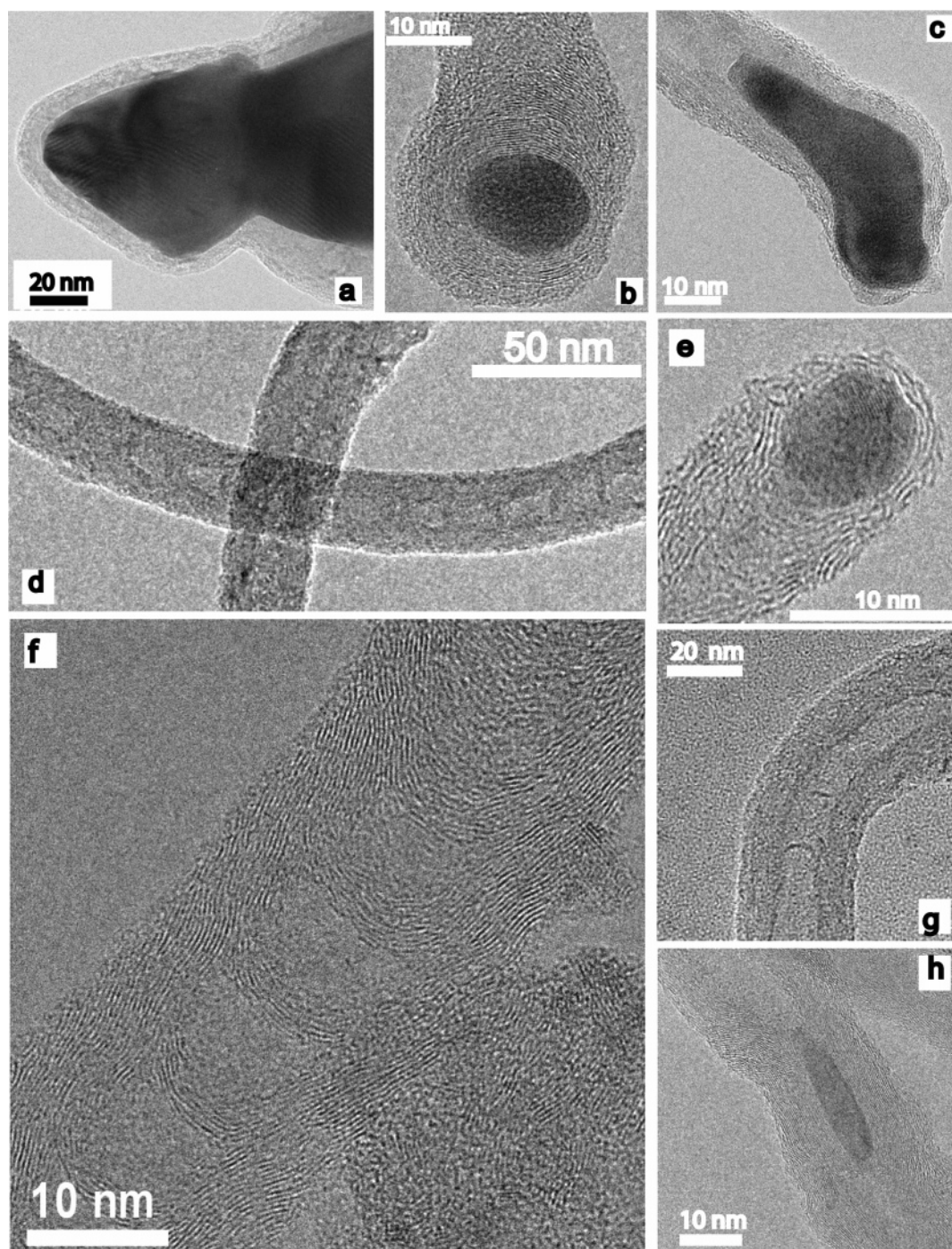


**Figure 8.** TEM images of metallocene-catalyzed MWNTs synthesized in supercritical toluene. The graphitic sheets generally are found folded around the metal seed particle, as shown in parts a–c and e (8.2 mM cobaltocene with 3.7 mM ethanol and 0.2 mM DI-H<sub>2</sub>O at 640 °C). Many of the tubes exhibited bamboo morphology, as shown in parts d, f, and g (625 °C, 8 mM nickelocene, 3.7 mM ethanol, and 0.2 mM DI-H<sub>2</sub>O). (h) In many cases, metal was found entrained in the middle of the nanotube as well (17 mM cobaltocene and 3.7 mM ethanol at 630 °C).

structure. Certainly, local temperature or reactant concentration fluctuations at the metal catalyst surface are possible in the supercritical toluene reactions.

### Conclusions

MWNTs were grown in supercritical toluene using ferrocene, cobaltocene, nickelocene, Fe, and Co nanocrystals as catalysts. A continuous flow reactor and cobalt and nickel precursors led to much higher yields than previous batch reactions in supercritical toluene. The addition of water significantly reduced amorphous carbon and nanofilament

formation. Additional reactive carbon sources such as hexane and ethanol gave higher MWNT yields. Cobaltocene was the best catalyst in terms of both the purity of the product and the conversion of toluene to nanotubes, which might be explained by higher carbon solubility into Co compared to Ni and Fe at temperatures of 600 to 650 °C. The nanotubes appear to grow by a folded growth mechanism. Many MWNTs exhibited significant defects in their graphitic layers, resulting in curly and kinked nanowires. In some cases, the nanowire bending was consistent along the length of the nanotube, resulting in coil, spring, and lasso structures.



In future work, conditions might be identified that will enable SWNT synthesis. However, the window of operating temperature is very limited. Reactions were carried out at the highest possible temperatures in our system ( $\sim 650^\circ\text{C}$ ), and as of yet, no SWNTs have been observed. Kanzow and Ding suggest that SWNT growth requires temperatures of at least  $900^\circ\text{C}$ ;<sup>50</sup> however, using catalytic CVD, Maruyama et al. reported the synthesis of SWNTs at temperatures as low as  $550^\circ\text{C}$ .<sup>24</sup> In the supercritical reactions, the relatively large size of the catalyst seeds may also be preventing SWNT formation.<sup>51–53</sup> Smaller metal seeds are needed to induce the extreme curvature of the graphitic sheets to form a SWNT, yet it is difficult to obtain and stabilize  $<2$  nm diameter metal

seeds in the very high-temperature solutions and may be another significant challenge facing SWNT growth in high-temperature supercritical solvents. Nonetheless, it seems possible that SWNTs could be produced in a supercritical organic solvent with the appropriate reactants and concentrations and this is an area of ongoing study.

**Acknowledgment.** This work was financially supported in part by the National Science Foundation (NSF) through their STC Program (CHE-9876674), the Robert A. Welch Foundation, and the Advanced Materials Research Center (AMRC) in collaboration with International SEMATECH, the Advanced Processing and Prototyping Center (DARPA: HR0011-06-1-0005), and the Office of Naval Research (N000N-05-1-0857). The authors are especially grateful to Aaron Saunders and Felice Shieh for synthesizing the Fe and Co nanocrystals used in the study and J. P. Zhou for TEM assistance.

CM060589M

(50) Kanzow, H.; Ding, A. *Phys. Rev. B* **1999**, *60*, 11180.

(51) Li, Y. M.; Kim, W.; Zhang, Y. G.; Rolandi, M.; Wang, D. W.; Dai, H. J. *J. Phys. Chem. B* **2001**, *105*, 11424.

(52) Li, Y.; Liu, J.; Wang, Y. Q.; Wang, Z. L. *Chem. Mater.* **2001**, *13*, 1008.

(53) Cheung, C. L.; Kurtz, A.; Park, H.; Lieber, C. M. *J. Phys. Chem. B* **2002**, *106*, 2429.